

Fermi Surface of the One-dimensional Kondo Lattice Model

S. Moukouri and L. G. Caron

Centre de recherche en physique du solide and département de physique,

Université de Sherbrooke, Sherbrooke, Québec, Canada J1K 2R1

(17 July 1996)

Abstract

We show a strong indication of the existence of a large Fermi surface in the one-dimensional Kondo lattice model. The characteristic wave vector of the model is found to be $k_F = (1 + \rho)\pi/2$, ρ being the density of the conduction electrons. This result is at first obtained for a variant of the model that includes an antiferromagnetic Heisenberg interaction J_H between the local moments. It is then directly observed in the conventional Kondo lattice ($J_H = 0$), in the narrow range of Kondo couplings where the long distance properties of the model are numerically accessible.

I. INTRODUCTION

Many experiments tell us that one of the low temperature states of the heavy fermion materials is a Fermi liquid whose quasiparticle masses are 10^2 to 10^3 larger than those of the normal metals [1]. It is commonly believed that the heavy Fermi liquid state is one of the possible ground states of the Kondo Lattice model (*KLM*). The most popular description of the heavy fermion state is that below a characteristic temperature T_{coh} ($T_{coh} \lesssim 10K$), the conduction electrons (*c*-electrons) and the local moments (*f*-electrons) have common excitations. This picture leads to the important fact that the localized spins also participate in the Fermi surface (*FS*). Thus, the *FS* has a large area. De Haas-Van Alphen measurements [2] of some heavy fermion compounds have shown that the *FS* has a *f* character. Ab-initio Local Density approximation (*LDA*) [3] computations of the band structure of heavy fermions also predict a large *FS*, although these calculations fail to reproduce heavy masses. These results are indeed expected from the Luttinger theorem which states that the volume of the *FS* is unchanged by the electron-electron interaction. Intuitively, however, it is not straightforward to understand in the framework of the *KLM*, how the *f*-electrons can be included in the *FS* since there is no explicit hybridization between the *c*-electrons and them. *LDA* computations have shown the existence of a narrow *f* bandwidth which is due to hybridization [4]. The *KLM* itself is an effective model of the periodic Anderson lattice (*PAM*) in the limit of nearly integral valence and of strong Coulomb correlation. One may thus wonder whether or not the residual *f*-electrons itinerant character present in the strong coupling limit of the *PAM* plays a crucial role in the formation of the heavy Fermi liquid state.

Analytical [5] [6] and numerical [7] [8] [9] studies have focused on the *FS* of the 1D *KLM*. Their results remain very controversial. In the following, we will study the 1D *KLM* numerically. A numerical study of the 1D *KLM* presents two essential difficulties. The first one arises from the very low energy scale of the Kondo physics which requires the investigation of lattices of very large sizes. In real materials, the heavy masses involve a very

small value of the quasiparticle weight. For the 1D model, in the physical range of parameters ($J_K \ll 1$), the size of the expected singularity in the electron momentum distribution $n_c(k)$ is likely to be very small. The second problem is the occurrence of a ground-state phase transition from a paramagnetic (*PM*) state at weak couplings to a ferromagnetic (*FM*) state at strong couplings [7] [9]. Therefore, the results of the strong coupling regime where the model converges more rapidly to the thermodynamic limit cannot be extrapolated to the weak-coupling region where size effects are still significant even in very long chains. We will show that the study of a *KLM* (Eq. 1) in which the strong coupling regime is smoothly connected to the weak coupling one can give insight of the existence of a large *FS* for the usual *KLM*. Then, a careful analysis of the usual *KLM* will be made. A large *FS* means that the Fermi wave vector is located at $k_F = k_{Fc} + \frac{\pi}{2}$, k_{Fc} being the Fermi wave vector of the *c*-electrons only. We will consider the following *KLM*:

$$H = -t \sum_{is} (c_{is}^\dagger c_{i+1s} + h.c.) + J_K \sum_i \mathbf{S}_{ic} \cdot \mathbf{S}_{if} + J_H \sum_i \mathbf{S}_{if} \cdot \mathbf{S}_{i+1f} \quad (1)$$

Where $\mathbf{S}_{ic}^\alpha = \frac{1}{2} \sum_{s,s'} c_{is}^\dagger \sigma_{ss'}^\alpha c_{is'}$ and \mathbf{S}_{ic}^α is a localized spin. The hopping integral t is set to 1. A direct Heisenberg exchange term between local moments J_H is introduced here. We have recently argued [9] that the occurrence of a ferromagnetic phase transition in the *KLM* in the strong coupling region is due to the fact that the *RKKY* interaction becomes ineffective. One would thus expect that a sufficiently strong antiferromagnetic Heisenberg coupling between the local moments can stabilize a *PM* ground state. In the conventional *KLM*, this term is usually omitted because typical lattice parameters in the heavy fermion compound are $3.5 - 4\text{\AA}$ while the ionic radii of the *f* ions are less than 1\AA , so that the overlap between the *f* orbitals is negligible. It should be noted that the strong J_K regime of the Hamiltonian (1) is relevant in the study of High- T_c materials. In this case, J_H is the superexchange interaction between copper ions. The double occupancy in the *c*-electron band is naturally suppressed by J_K , so that one need not include an explicit repulsion term between these electrons. We have investigated Hamiltonian (1) using the density matrix renormalization group (*DMRG*) method [10]. We have chosen an algorithm with open

boundary conditions. We keep between 64 and 150 states in the two external blocks. These states are labelled by the z -component of the total spin S_T^z . The ground state corresponds to the lowest state with $S_T^z = 0$. The maximum truncation error is in the order of 10^{-4} . Although we have reached $N = 60$ sites, the longest distance in the calculation of the correlation function is $L = 22$. Because we have first built lattices of 20 sites before we start to calculate the correlation functions. This way, we minimize the end effects and density fluctuations that are larger in the early steps of the algorithm.

II. RESULTS FOR THE KONDO-HEISENBERG CASE ($J_H \neq 0$)

The Hamiltonian (1) has a *PM ground state with a Luttinger Fermi surface* when $J_H = 0.5$ in the strong J_K regime. We have chosen our value for the Heisenberg coupling on the grounds that it is necessary that J_H exceeds the effective *FM* coupling J_{eff}^{\max} between the f electrons to stabilize the *PM* ground state for all J_K . Our first choice was $J_H = 0.1$. For this value, we found that the ground state is *PM* in the weak J_K region, *FM* for intermediate couplings, then *PM* for strong J_K . We can estimate J_{eff} by using the results of the strong coupling expansion [11]. $J_{eff}J_K/t^2$ is approximately 0.05, 0.2 and 0.25 respectively for the partial band-fillings $\rho = 0.25, 0.5$ and 0.75 . Then, knowing that the strong coupling region starts for J_K of order 1, one obtains the upper bound, $J_{eff}^{\max} \simeq 0.25$ for $t = 1$. Our value of 0.5 thus include a security factor. In Fig.1, we show $n_c(k)$ (the Fourier transform of $\langle c_{i\sigma}^\dagger c_{j\sigma} \rangle$) for the band-fillings $\rho = 0.25, 0.5$ and 0.75 for $J_K = 10$. $n_c(k)$ at 0.25 and 0.75 are affected by density fluctuations, since the band-filling is not constant during the *DMRG* iterations. Nevertheless, clean singularities are observed at $k_F = 0.625\pi, 0.75\pi$ and 0.875π . The magnetic structure factor of the localized electrons $S_f(k)$ (the Fourier transform of $\langle S_{if}^z S_{jf}^z \rangle$), shown in Fig.2, presents a maximum at $2k_F = 0.75\pi, 0.5\pi$ and 0.25π respectively. These values correspond to $2\pi - 2k_F$, since $2k_F$ is greater than π . Clearly, neither the bare c -electron nor the bare f -electron signatures are detected. There are instead unique compound-particles propagating with a characteristic wave vector at k_F . An

analogy can be made with the Hubbard model [12]. At half-filling, in the $J_K = \infty$ limit, all the conduction electrons form on-site singlets with the localized spins, so that the overall system is in a singlet state. The non half-filled cases correspond to the introduction of holes in the system. These holes which can hop from site to site are associated with the $N - N_c$ unpaired f -electrons, N_c being the number of c -electrons. Obviously, double occupancy of holes is forbidden : one has a $U = \infty$ Hubbard model of $\rho_h = 1 - \rho$ hole density. Depletion effects [13] are also observed in Fig.2: the reduction of the conduction electron density increases the tendency to magnetism. The maximum of $S_f(k)$ increases when ρ decreases.

Now we wish to discuss how the system evolves when J_K is reduced. We show in Fig.3 $n_c(k)$ at $\rho = 0.5$ for $J_K = 10, 8, 6, 4, 3, 2.5$ and 2. The height of the singularity at k_F decreases as J_K is reduced. Concurrently the drop at k_{Fc} which, was negligibly small in the strong J_K case, increases. The c -electron character is progressively enhanced. The local spin-spin correlation which is $\langle S_{ic}S_{if} \rangle = -.3748 \simeq -\frac{3}{4}\rho$ at $J_K = 100$, is equal to $-.366$ at $J_K = 10$ and $-.183$ at $J_K = 2$. The deviation of this quantity from the perfect on-site singlet value $-\frac{3}{4}\rho$ means that the singlet clouds have a spatial extension at lower J_K . At $J_K = 2$, short-range effects coexist along with the long-range behavior of the system. Clearly, it becomes hard to define the exact position of the FS . This can be better illustrated in $S_f(k)$ (Fig.4) at $\rho = 0.5$. A new peak appears at $k = \pi$ at small J_K , signaling short-range antiferromagnetic correlations. At $J_K = 1.5$ (not shown here), the peak at $2k_F$ is not seen. We can no longer observe the long-distance behavior of the model because of the finite-size effects (long correlation length; see the discussion below). Since there is no phase transition in the system, the weak and the strong J_K regimes are continuously connected. We thus believe that *the FS is large even at smaller J_K* . The above discussion is similar to the one made by Kotliar in the framework of the *PAM* [14]. The local singlets of the strong-coupling limit are obtained as the Kondo resonances are pulled out of the c -electron band by increasing J_K . The FS is conserved during this process.

III. RESULTS FOR THE CONVENTIONAL KLM ($J_H = 0$)

We now discuss if the above conclusions can be extended to the *PM* phase of the conventional *KL**M*. At first sight, one can argue that the conventional *KL**M* is adiabatically reached by taking the limit $J_H \rightarrow 0$. Thus the conventional *KL**M* may have a large *FS* in its *PM* phase. It should be noted from the above results and from the knowledge of the occurrence of a phase transition, that the range of J_K in which we can expect to detect a large *FS* with numerical methods in the conventional *KL**M* is narrow. An estimation of this range can be obtained by examining the Kondo coherence length ξ_K of the one-impurity problem. $\xi_K = v_F/T_K$, where v_F is the Fermi velocity and T_K the Kondo temperature. The observation of the long range properties of the model is only possible at distances $r \gg \xi_K$. For $r \lesssim \xi_K$ finite size effects dominate, only short-range effects governed by the *RKKY* interaction will be observed. Sørensen and Affleck have recently made an accurate computation of ξ_K [15]. Some typical values are $\xi_K = 1, 2, 4.85, 8$ and 23 for $J_K = 2.5, 2, 1.5, 1.25$ and 1 respectively. Clearly, for $J_K \lesssim 1.25$ the long-range behavior of the model is not attainable since the longest distance in our study is $L = 22$. Moreover, the *FM* transition occurs at $J_K \simeq 1.5$ for $\rho = 0.5$ and $J_K \simeq 2.75$ for $\rho = 0.75$. At low band-fillings, depletion effects enhance the *FM* instability. The *PM* phase boundary is shifted towards weak couplings where ξ_K becomes very large. Hence, at quarter filling where there is no density fluctuations, this range is very narrow. Thus we have chosen to study the *KL**M* at $\rho = 0.75$ in the range $1.25 \lesssim J_K \lesssim 2.5$. In Ref. [9], we have found that $n_c(k)$ displays a sharp drop at k_{Fc} and $S_f(k)$ presents a maximum at $2k_{Fc}$ in the small J_K regime. As J_K was increased, these features vanished before the phase transition was reached. But we were unable to draw a firm conclusion about the location of the *FS*. A more careful analysis will now show that we had observed a short-range effect governed by the *RKKY* interaction. Furthermore, we will identify the true long-range properties of the model which are not easily observable. In Fig.5, we display $S_f(k)$ at $\rho = 0.75$ for $J_K = 1.25, 1.5, 1.75, 2$, and 2.5 . Starting from $J_K = 1.25$, we can only detect the *RKKY* maximum at $2k_{Fc} = 0.75\pi$. For $J_K = 1.5$, the

maximum of $S_f(k)$ is still located at the *RKKY* wave vector. But one can also observe a local maximum at the position of the large *FS* at $2k_F = 0.25\pi$. At $J_K = 1.75$ and 2 , the height of the *RKKY* maximum decreases. At the same time, the height of the maximum at $2k_F$ increases. This trend is unambiguously confirmed at $J_K = 2.5$, where the maximum at $2k_F$ is now the highest. The height of these maxima however, is still smaller than the one at $2k_{F_c}$ for $J_K = 0.5$ in ref [9], and are thus harder to detect. Finally, $n_c(k)$, shown in Fig.6, corroborates the existence of the large *FS* in the *KLM*. $n_c(k)$ drops monotonously when $k < k_F = 0.875\pi$, shows a small plateau just before $k = k_F$, and then drops abruptly at $k \simeq k_F$. The width of the plateau shrinks and then becomes undetectable when J_K is decreased. At the same time, the drop at k_{F_c} is enhanced indicating that the short range effects are becoming dominant. This is consistent with the results for $S_f(k)$.

IV. CONCLUSION

In summary, we have shown that the *KLM* with a direct exchange Heisenberg coupling has a large *FS* in the strong Kondo coupling limit. We have shown that this phase is continuously connected to the weak Kondo coupling regime. As a consequence, the latter model has a large *FS* in the small coupling regime. The conventional *KLM* can continuously be reached by taking the limit of vanishing Heisenberg coupling. We have concluded from this that its *FS* should have a large area in its *PM* phase. Direct numerical computations made on the *KLM* support the existence of a large *FS*. The height of the singularity in the electron momentum distribution decreases and becomes very small as the Kondo interaction goes towards the weak coupling region. These features are however very hard to observe. A more accurate study is certainly needed to confirm our conclusions. Finally, the nature of the heavy quasiparticles appear to be different from that proposed in the renormalized band structure studies [16]. In the renormalized band picture, the heavy quasiparticles result from the small hybridization between the conduction electrons and the renormalized *f*-bands pinned at the Fermi level of the conduction electron sea. This requires the number

of f -electrons per site to be slightly less than one. Our results suggest that these are instead loosely bound states made up of conduction electrons and f -spin fluctuations. This is consistent with recent results from field theory [17] and exact diagonalization [18].

We wish to thank S. Fujimoto for indicating ref. [6] to us. This work was supported by a grant from the Natural Sciences and Engineering research Council (NSERC) of Canada and the Fonds pour la formation de Chercheurs et d'Aide à la Recherche (FCAR) of the Québec government.

REFERENCES

- [1] G. R. Stewart, Rev. Mod. Phys. **56**, 755 (1984).
- [2] W. R. Johanson, G. W. Crabtree, A. S. Edelstein and O. D McMasters, J. Magn. Magn. Mat. **31-34**, 377 (1983).
- [3] D. D. Koelling, Solid State Commun. **43**, 247 (1982); A. Yanase, J. Magn. Magn. Mat. **31-34**, 453 (1983).
- [4] A. M. Boring, R. C. Albers, F. M. Mueller and D. D. Koelling, Physica **130B**, 1711 (1985). R. C. Albers, Phys. Rev. B **32**, 7646 (1985).
- [5] P. Fazekas and E. Müller-Hartmann, Z. Phys. B **85**, 285 (1991).
- [6] S. Fujimoto and N. Kawakami, J. Phys. Soc. Jpn **63**, 4322 (1994).
- [7] H. Tsunetsugu, M. Sigrist and K. Ueda, Phys. Rev. B **47**, 8345 (1993).
- [8] K. Ueda, T. Nishino and H. Tsunetsugu, Phys. Rev. B **50**, 612 (1994).
- [9] S. Moukouri and L. G. Caron, Phys. Rev. B **52**, 15723 (1995).
- [10] S. R. White, Phys. Rev. Lett. **69**, 2863 (1992); Phys. Rev. B **48**, 10435 (1993).
- [11] M. Sigrist, H. Tsunetsugu, K. Ueda and T. M. Rice, Phys. Rev. B **46**, 13838 (1992).
- [12] C. Lacroix, Solid State Commun. **54**, 91 (1985).
- [13] P. Nozières, Ann. Phys. (Paris) **10**, 19 (1985). L. G. Caron and C. Bourbonnais, Europhys. Lett. **11**, 473 (1990). S. Moukouri, Liang Chen and L. G. Caron, (unpublished).
- [14] G. Kotliar, Int. J. Mod. Phys. B **5**, 341 (1991).
- [15] E. S. Sørensen and I. Affleck, (unpublished), Preprint-no : *IUCM* – 95046.
- [16] C. Lacroix and M. Cyrot, Phys. Rev. B **20**, 1969 (1979); T. M. Rice and K. Ueda, Phys. Rev. Lett. **55**, 995 (1985); B. H. Brandow, Phys. Rev. B **33**, 215 (1986).

- [17] A. M. Tsvelik Phys. Rev. Lett. **72**, 1048 (1994).
- [18] K. Tsutsui, Y. Ohta, R. Eder, S. Maekawa, E. Dagotto and J. Riera, Phys. Rev. Lett. **76**, 279 (1996).

FIGURES

FIG. 1. The electron momentum distribution $n_c(k)$ for $\rho = 0.75, 0.5$ and 0.25 at $J_K = 10$ and $J_H = 0.5$.

FIG. 2. The magnetic structure factor $S_f(k)$ for $\rho = 0.75, 0.5$ and 0.25 at $J_K = 10$ and $J_H = 0.5$.

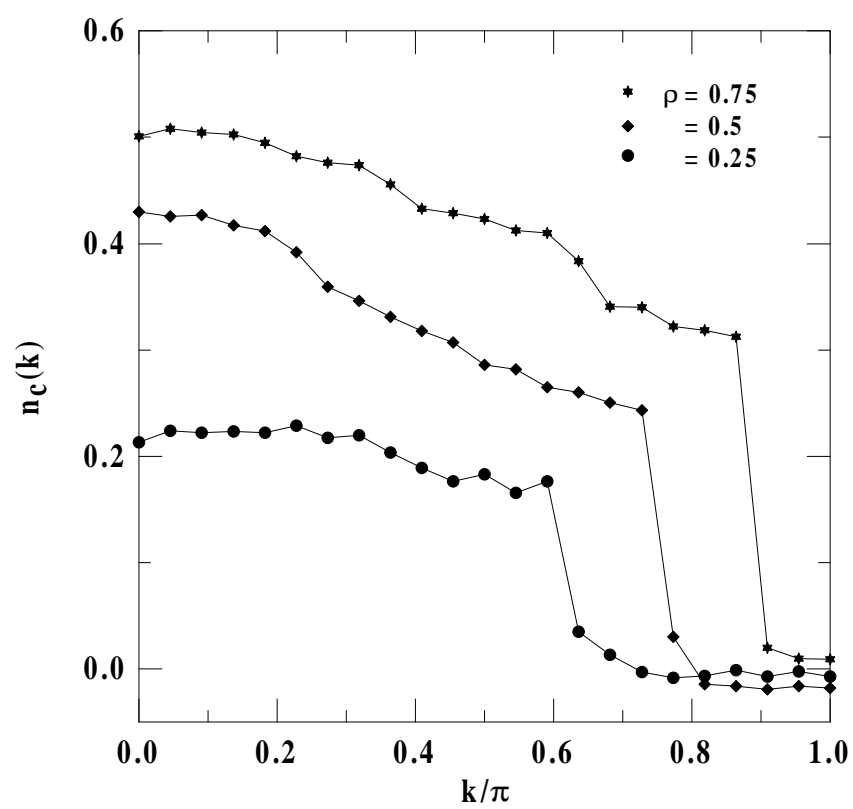
FIG. 3. $n_c(k)$ for various values of J_K at $\rho = 0.5$ and $J_H = 0.5$.

FIG. 4. $S_f(k)$ for various values of J_K at $\rho = 0.5$ and $J_H = 0.5$.

FIG. 5. $S_f(k)$ for $J_K = 1.25, 1.5, 1.75, 2$ and 2.5 at $\rho = 0.75$ and $J_H = 0$.

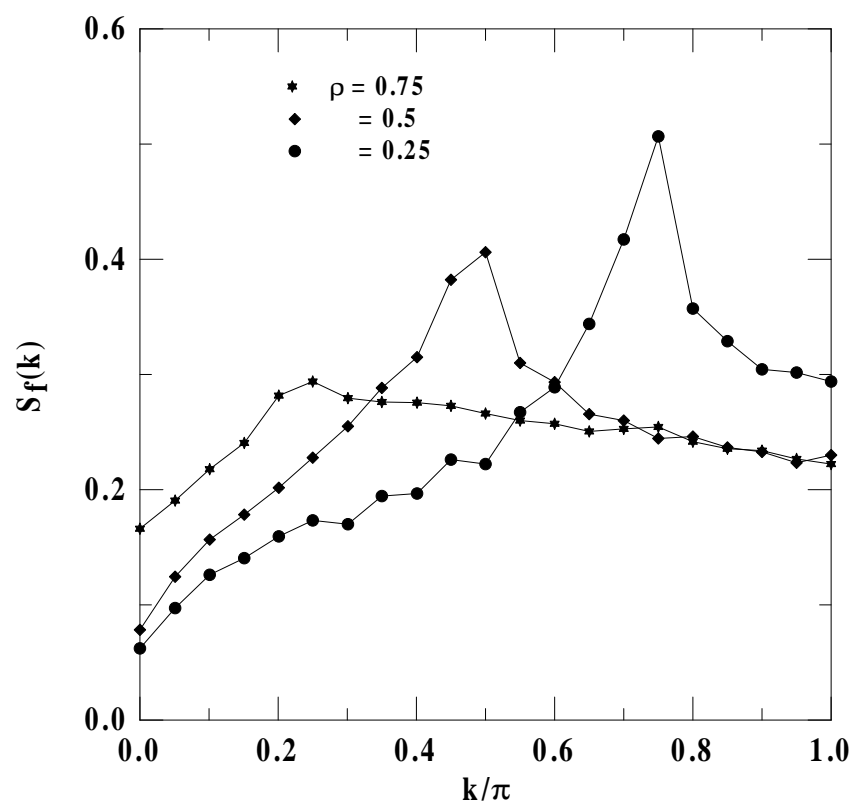
FIG. 6. $n_c(k)$ for $J_K = 1.5, 2$ and 2.5 at $\rho = 0.75$ and $J_H = 0$.

Fig. 1



Moukouri and Caron

Fig. 2



Moukouri and Caron

Fig. 3

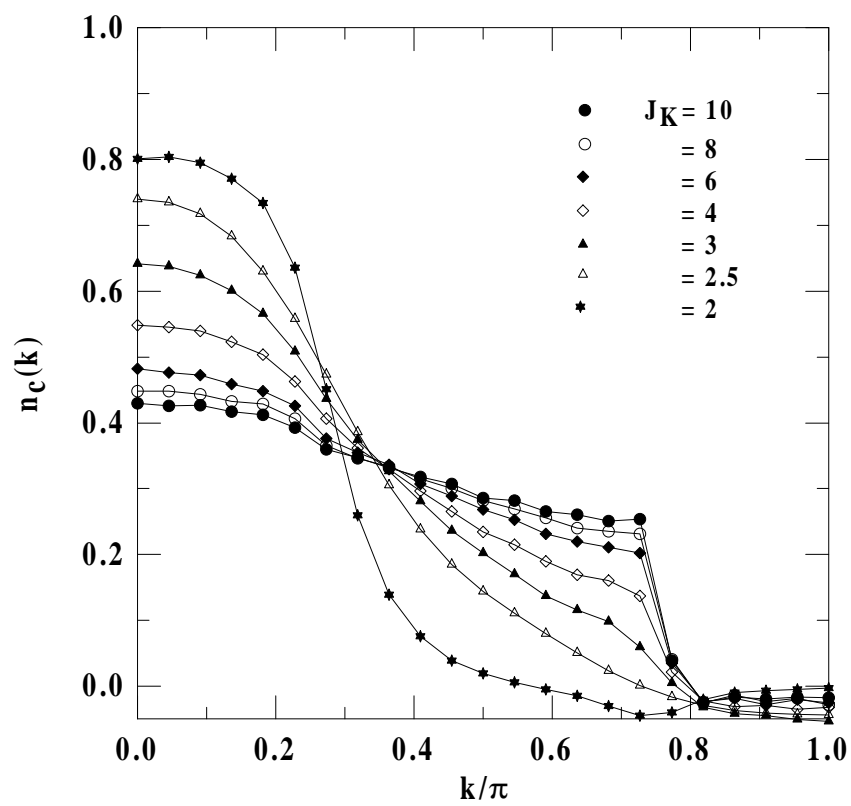


Fig. 4

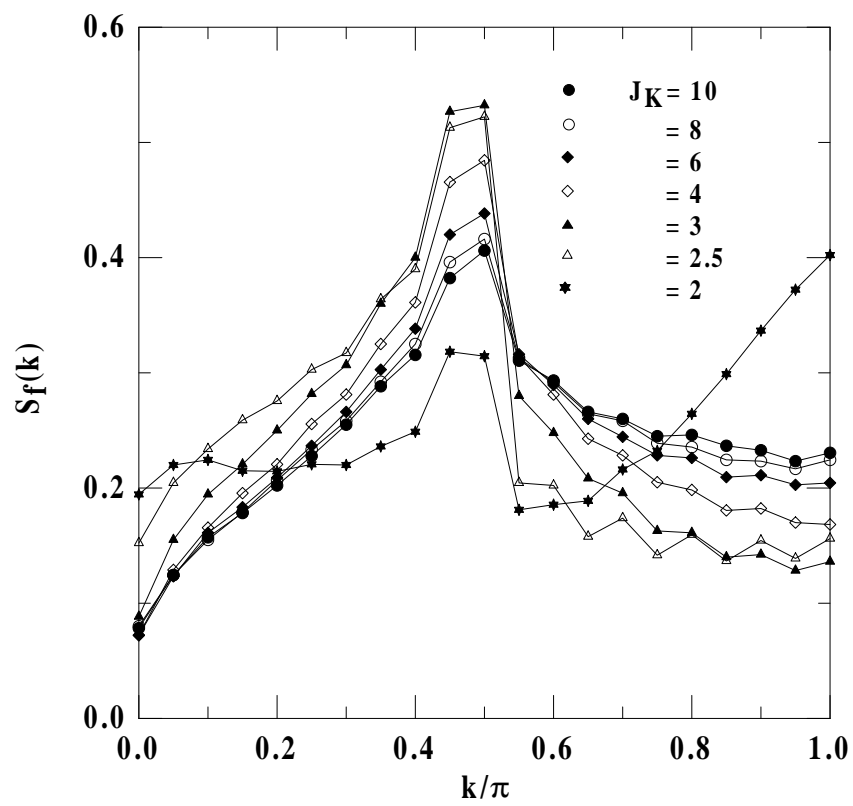


Fig. 5

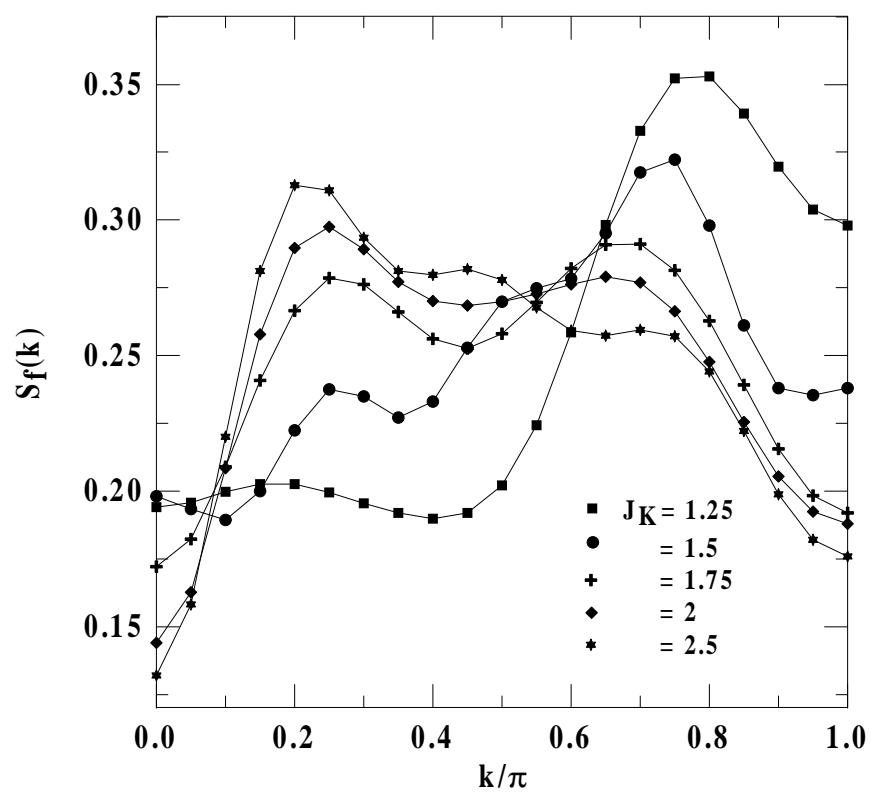


Fig. 6

